ROZPRAWY INŻYNIERSKIE • ENGINEERING TRANSACTIONS • 29, 1, 5—26, 1981
Polska Akademia Nauk • Instytut Podstawowych Problemów Techniki

SIMPLIFIED CRUSHING ANALYSIS OF THIN-WALLED COLUMNS AND BEAMS

W. ABRAMOWICZ (WARSZAWA)

An approximate method is developed for calculating the strength and energy absorption of thin-walled beams and columns with rectangular, square, closed-hat and "u" shape cross sections. Three basic deformation mechanisms are distinguished and the mean crushing force and bending resistance is determined. The present solution is compared with existing experimental data. In all cases good agreement is obtained.

1. INTRODUCTION

The purpose of this paper is to develop approximate formulae for the crushing strength and energy absorption of thin-walled columns and beams with various shapes of the cross section. A direct motivation for undertaking the present research was to get more accurate prediction of the response of major components of motor vehicles, buses, trains, aircrafts and ships during collisions.

When a thin-walled structure is subjected to compressive loads, usually the loss of stability takes place either in the elastic or plastic range. Slender columns buckle globally (Euler instability) while in shorter columns or beams local buckling is observed. In this paper we shall be concerned only with local forms of plastic instability. Plastic deformations are not spread uniformly over the buckling zones but are confined to rather narrow strips, called hinge lines, where strains and strain rates usually reach high magnitudes. Depending upon the degree of symmetry and loading conditions, a more or less regular pattern of wrinkles and folds is formed. The overall behaviour of local plastic buckling can be conveniently described through a kinematic approach, i.e. assuming a certain collapse mechanism. The collapse mechanism usually involves one or several free parameters which are then determined from the postulate of minimum plastic work or minimum external force. A rigid-perfectly plastic material idealization is introduced and the Tresca yield condition is used.

There is extensive literature [1, 2, 3, 4, 12, 13, 14] concerning compression of thin-walled columns with rectangular, square and hat cross-sections (Fig. 1). Similar experiments on bending of closed-section beams were reported in Ref. [5, 6, 14, 15]. Corresponding tests on open section beams do not appear to have been published. The present author performed a preliminary series of experiments [9] in which the *u* section beams (Fig. 2) were subjected to bending in two directions. These

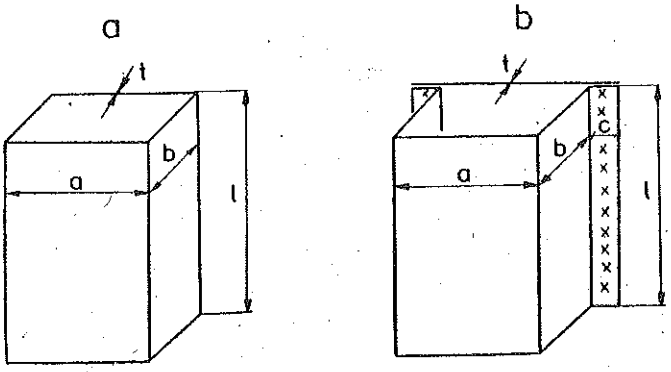

FIG. 1. Types of test pieces.

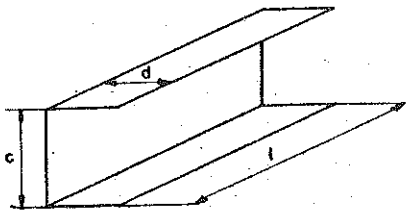

FIG. 2. *U*-section beam, notation.

tests were aimed at determining the mechanism of local plastic collapse; the moment--rotation characteristics at the generalized plastic hinge were not recorded.

The observed crumpling mechanism is used in this paper to obtain a new approximate solution for the bending resistance of *U*-section beams. Also, existing solutions concerning bending and compresion of closed section members are revised and improved to get a unified treatment of the crumpling process of a whole class of structural members used in engineering practice.

2. LOCAL BUCKLING MODES IN THIN-WALLED CRUSHED MEMBERS

2.1. General considerations

Consider first a box section member crushed between parallel plates. For a sufficiently long member the deformation process proceeds progressively. Once the first fold is formed either by a natural plastic buckling or pre-buckling process (Fig. 3), then the member continues to collapse in the same manner and with the same wave length ($2h$) as the panel that first buckled (Fig. 4). This collapse mode is a function of section configuration (see Fig. 5). In all experiments on box section members performed by the present author [12], the wave length ($2h$) was found to be equal approximately to one quarter of the length of the shorter side $h=b/4$. This observation agrees with the results reported in the literature [1, 3].

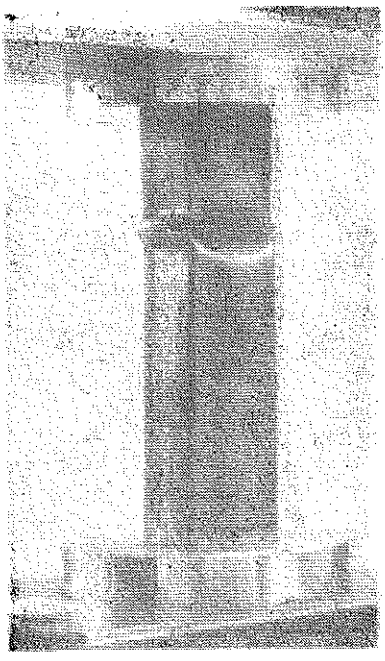

FIG. 3. Formation of the first fold in crushed thin-walled metal column.

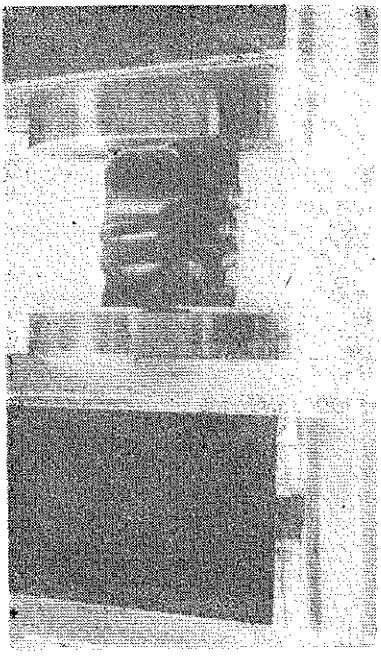

FIG. 4. Partially crushed thin-walled metal column.

FIG. 5. Typical collapse modes of columns with various cross sections.

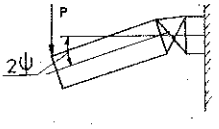

FIG. 6. Bending process of beam clamped at one end.

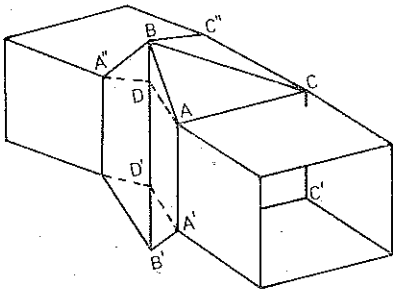

FIG. 7. Collapse mechanism of the closed-section rectangular column.

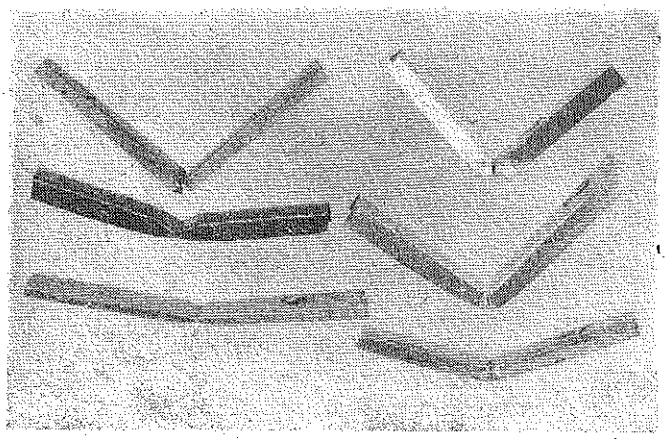

FIG. 8. Final shapes of local buckling process of *U*-section beams ("inward bending").

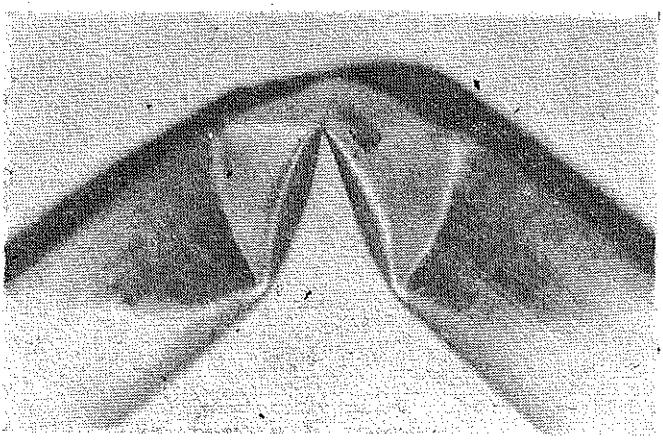

FIG. 9. Generalized plastic hinges in "inward bending".

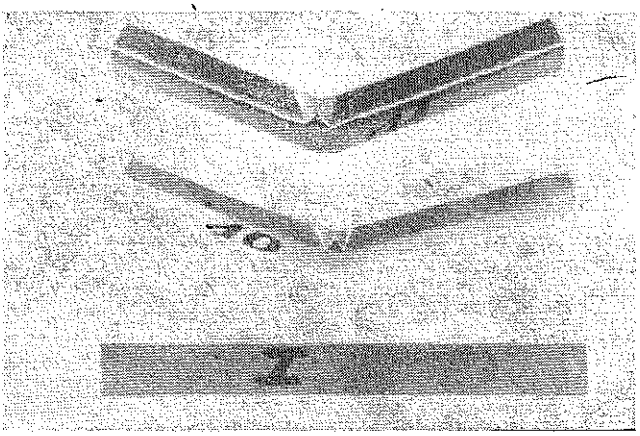

FIG. 10. Final shapes of local buckling process in *U*-section beams ("outward bending").

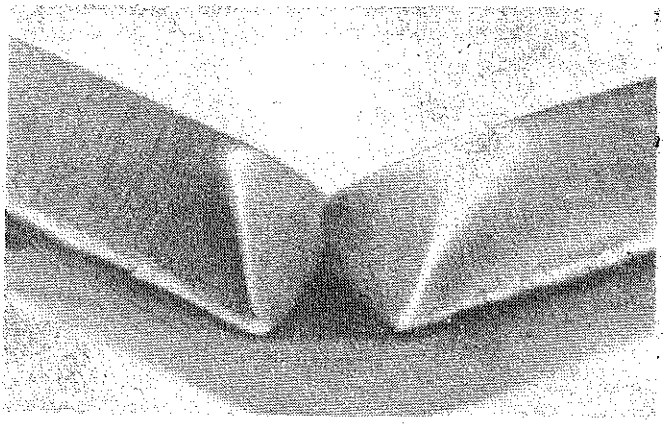

FIG. 11. Generalized plastic hinges in "outward bending".

In the bending process of beams clamped at one end and subjected to the concentrated force at the other one (Fig. 6.), plastic deformations are confined to a rather narrow portion of the beam where the so-called generalized hinge is formed. The collapse mechanism of closed-section rectangular columns suggested by experiments is shown schematically in Fig. 7.

It should be noted that some authors proposed more complicated kinematics of the local buckling process (see ref. [5, 6]); the resulting analysis is, however, much more complicated and does not introduce any noticeable improvement to the theory.

In the bending process of open section members one has to distinguish between two directions of bending. By "inward bending" we understand bending of a *U*-section beams in which the web is subjected to tension.

In the "inward bending" of *U*-section beams a similar shape of local buckling as in closed section-beams is observed, (Fig. 8). A more detailed picture of the location of plastic hinges is shown in Fig. 9.

Bending in the opposite direction, called an "outward bending", produces a very simple collapse mechanism where the positions at plastic hinges are shown in Figs. 10 and 11.

2.2. Kinematics of the collapse process of columns and beams

The crushing process of shell structures is in general quite complicated. As shown in the preceding section compressed columns and bent beams exhibit locally various forms of plastic buckling. One can distinguish several characteristic features of the collapse process of thin shells, the most important ones are:

(i) Formation of localized zones of plastic flow along the so-called hinge lines.

(ii) Variable position of hinge lines. The hinge may travel leaving a complicated pattern of folds with sharp changes of curvature, or may stay in the same position during the whole process.

(iii) Each separate fold line lies always in a certain plane and remains in it as the deformation process goes on.

(iv) The bending deformation is predominant with very little extension of the shell middle surface. Thus the inextensibility of the deformation can be assumed, which in terms of mathematics can be referred to as an isometric transformation of a middle surface of the shell.

The foundations of the respective mathematical theory were laid by POGORIELOV [10, 11]. The formalism developed by this author appears to be particulary suited for analysing the crumpling process of shell-structures. In the present paper a simple class of isometric transformations of middle surface is introduced. This transformation consists of a system of stationary and moving straight hinge lines and plane trapezoidal, triangular and rectangular surface elements. Examples of isometric transformations and general geometrical relations of the already mentioned structures are shown in Figs. 7 and 12–16. Figure 12 presents an isometric model of the progressive crushing of a column with a hat-cross section (there only a part of the column with a length $2h$ is presented).

The lines ab, bc, $a'b'$, $b'c'$, etc. are stationary hinge lines while lines $2b'$, $1a'$, etc. are the moving hinge lines.

Figure 13 presents three stages of the collapse of columns with square and rectangular cross sections. The only difference here is that point 3 moves in an opposite direction than in hat sections.

Figure 14 shows an intermediate stage of the crushing process of columns and describes the notation used. The following relations follow from the kinematic considerations:

$$|\overline{B'B_1'}|=h\sin\Theta, \tag{2.1}$$

$$\sin\Theta=\operatorname{tg}\Psi, \tag{2.2}$$

$$\delta=2h(1-\cos\Theta). \tag{2.3}$$

An idealization of the bending of a beam with closed cross sections is presented in Fig. 7. Here the segments AC, $A''C''$, CC'', etc. represent stationary hinge lines, while the segments AB, $A''B$, BC, BC'', etc. are moving hinge lines.

The same mechanism is activated in the "inward bending" of U-section beams (see Figs. 9 and 15). The geometrical parameters are related by

$$\cos\Phi=1-2\lambda\sin\Psi, \tag{2.4}$$

$$\alpha=\Phi-\Psi, \quad \text{where} \quad \lambda=a/b. \tag{2.5}$$

In the case of the "outward bending" of a U-section beam only stationary hinge lines are formed (Fig. 16). From the assumed mechanism of local buckling it is easy to derive the relations between α, β, φ, and $\tilde{\Phi}$

$$\cos\beta=\left(\frac{1}{2\sin 2\alpha}-\operatorname{tg}\alpha\right)\operatorname{tg}\left(\alpha-\frac{\varphi}{2}\right), \tag{2.6}$$

$$\sin\left(\frac{\tilde{\Phi}}{2}\right)=\operatorname{ctg}\alpha\operatorname{tg}\left(\alpha-\frac{\varphi}{2}\right). \tag{2.7}$$

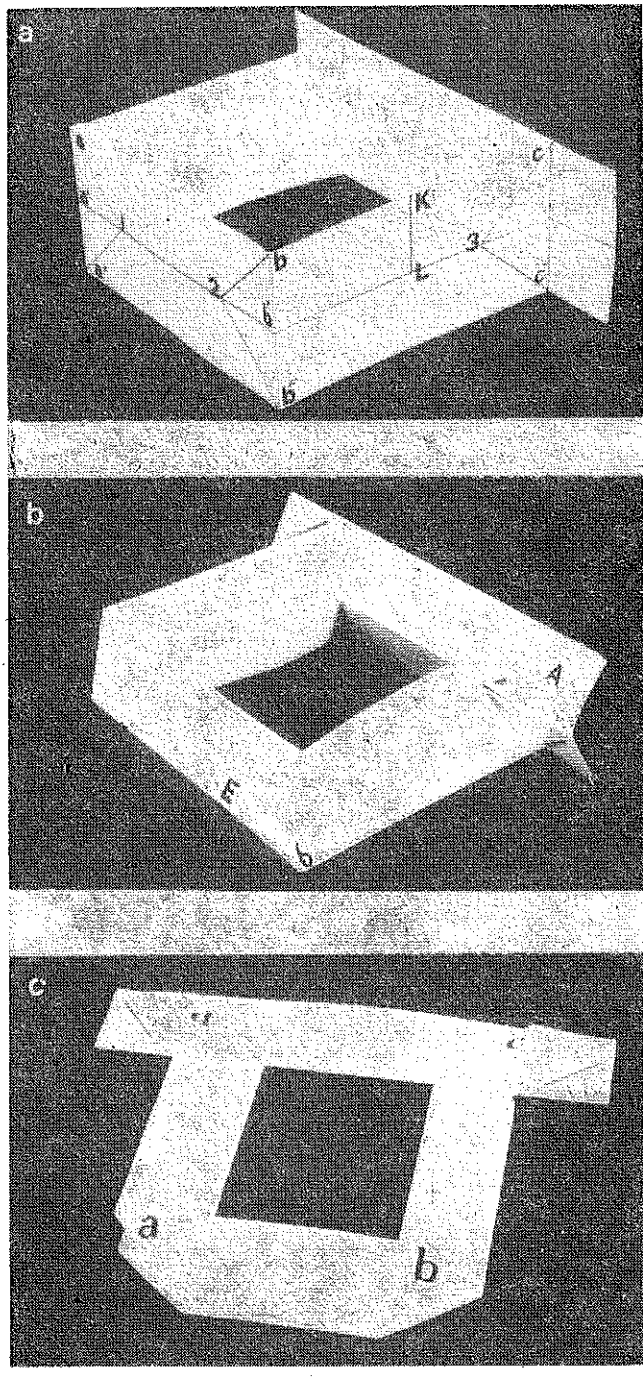

FIG. 12. Isometric models of the progressive crushing of hat section column.

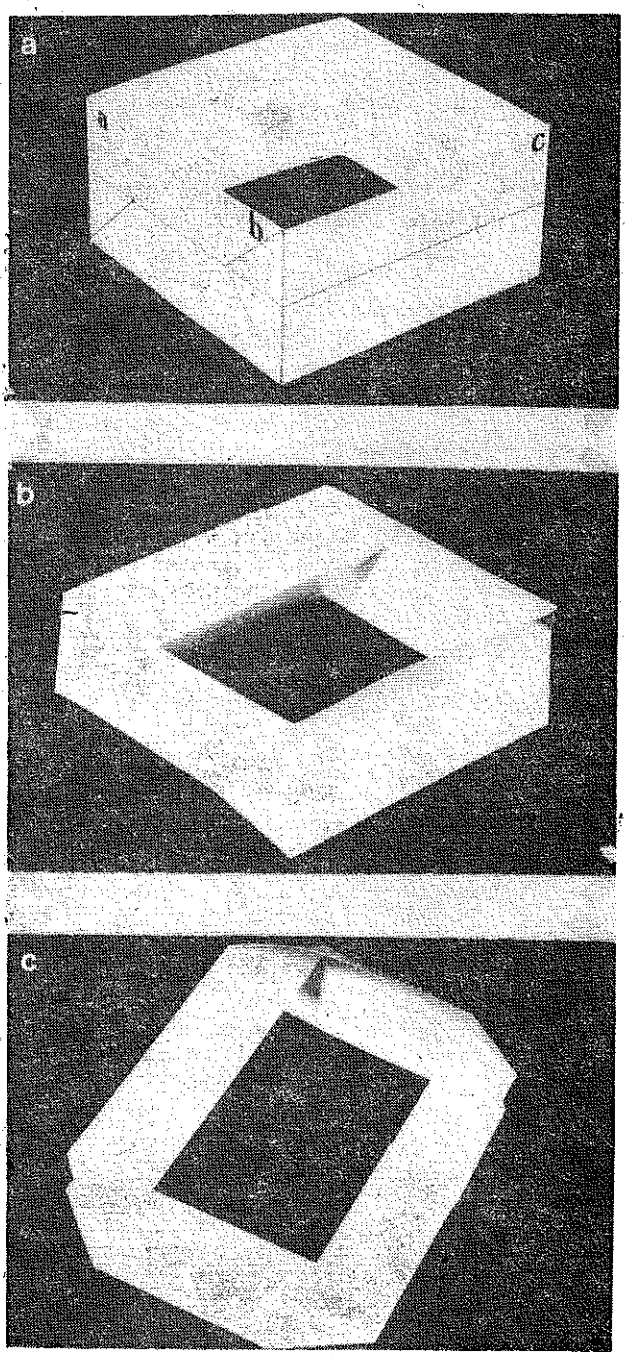

FIG. 13. Isometric models of the progressive crushing of square section column

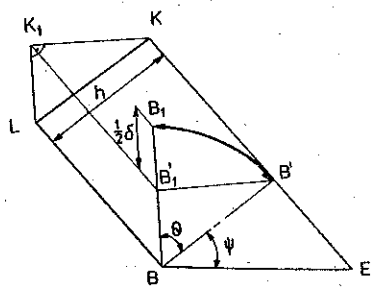

FIG. 14. An intermediate stage of the crushing process of columns (one quarter of the column side).

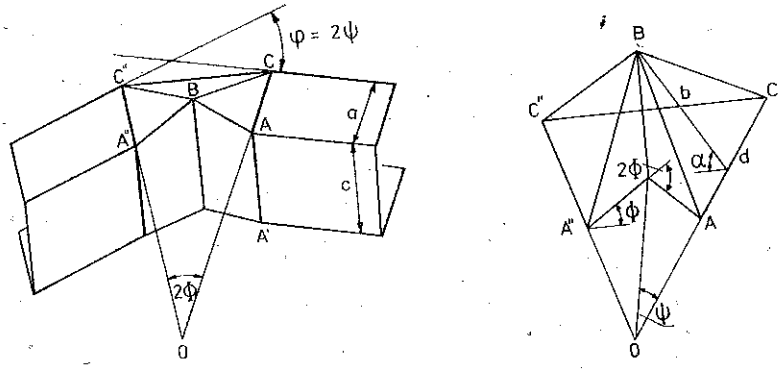

FIG. 15. Collapse mechanism of "inward bending" of *U*-section beam.

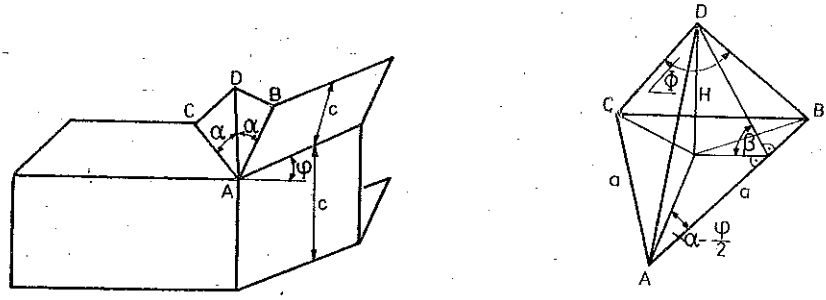

FIG. 16. Collapse mechanism of *U*-section beam ("outward bending").

3. BASIC MECHANISMS OF ENERGY DISSIPATION IN THE LOCAL PLASTIC BUCKLING

In the collapse process of a shell structure described by isometric transformations of the middle surface, it is possible to distinguish three basic mechanisms of plastic deformations and write down expressions for the corresponding rates of energy dissipation:

(i) Bending about stationary hinge lines. The corresponding rate of energy dissipation is

$$dE_b = M_0\, d\Theta l, \tag{3.1}$$

where $M_0=(\sigma_0 t^2)/4$ is a fully plastic moment per unit length, σ_0 is the yield stress of the material and t denotes the wall thickness; Θ is the rotation angle and l denotes the length of hinge (in general l may be a function of Θ or other parameters).

(ii) Bending about moving hinge lines is frequently called the rolling type of deformations (Fig. 17). The corresponding rate of energy dissipation is

$$dE_r=2M_0\frac{dS}{R}, \tag{3.2}$$

in which R is the rolling radius and S denotes the area of the rolling strip. Details of calculations are given in Ref. [8].

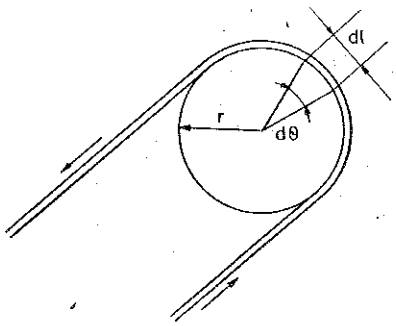

FIG. 17. Mechanism of the rolling deformation.

(iii) Reverse bending (corner deformation). It is seen from Fig. 18 that when the corner point is advanced through an infinitesimal distance dx, the side panels are bent through an angle $\gamma=\gamma_1-\gamma_2=4\Theta$ (Fig. 19). The corresponding rate of energy dissipation is equal to

$$dE_{cb}=M_0\,\gamma dx\,. \tag{3.3}$$

This type of middle surface isometric deformation was first described by N. AYA *et al.* [2] in 1973. It is a first attempt to describe the complicated mechanism of corner deformation which actually is not isometric.

The assumption about the constant rolling radius along the moving hinge lines is clearly not compatible with the assumed inextensible deformation of the corner. The purely inextensible deformation mode inevitably leads to the material discontinuity at the corner point.

Work is in progress to take into account the extension of the shell middle surface during the advancement of two adjacent hinge lines. Clearly, the shell extensions result in a dissipation of some additional energy. Thus the present analysis which completely ignores stretching deformations must underestimate the dissipated plastic work.

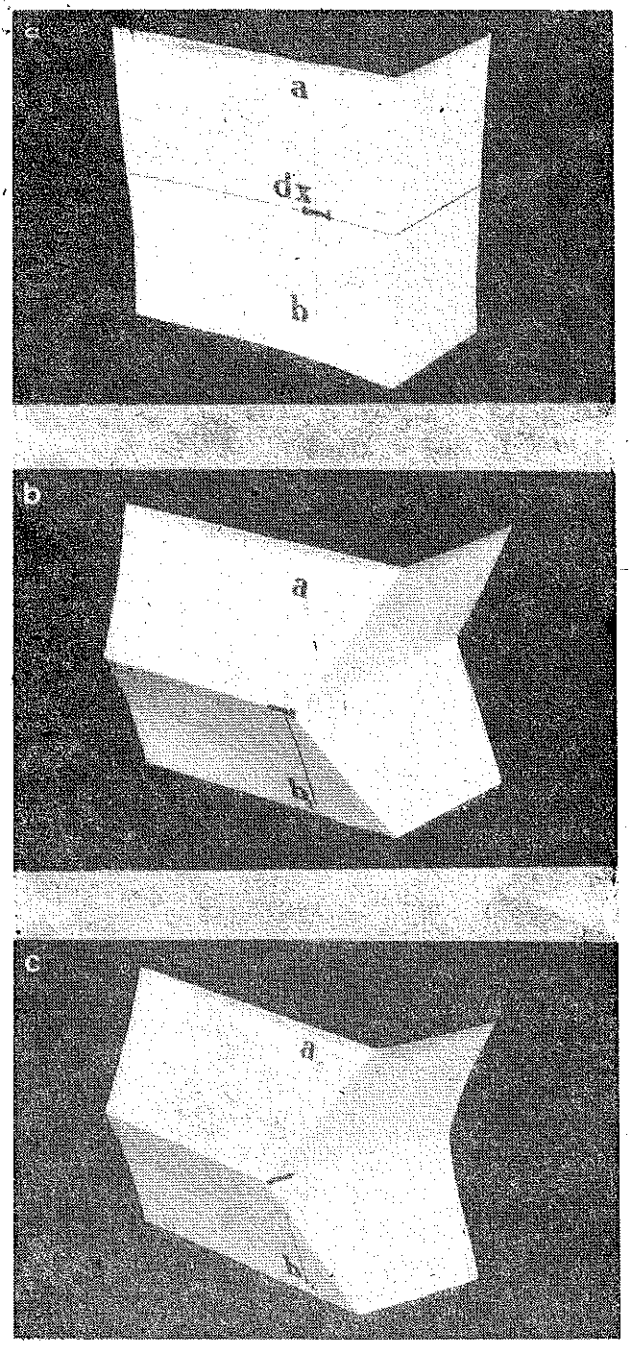

FIG. 18. Mechanism of the corner deformation.

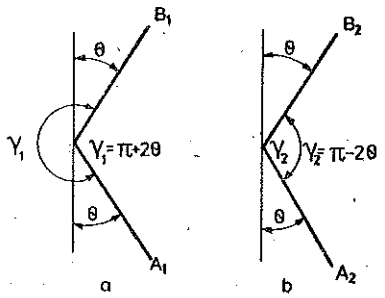

FIG. 19. Bending of side panels during corner deformation.

4. MEAN CRUSHING STRENGTH OF COLUMNS

The energy dissipated during the crumpling of the column (E_c) is a sum of energies due to bending, rolling and corner deformation. Since the formation of local buckles is repeatable, it suffices to consider only one wave-length, thus:

$$E_c=\int_0^h dE_b+\int_0^h dE_r+\int_0^h dE_{cb}. \tag{4.1}$$

Using Eqs. (3.1)-(3.3), it is easy to calculate E_c in the particular cases of various cross sections of columns ([1]). For columns with a hat-sections

$$E_c=M_0\left[2\pi(a+b+4c)+\frac{4h^2}{R}+5\pi h\right], \tag{4.2}$$

for the columns with square and rectangular cross sections:

$$E_c=M_0\left[2\pi(a+b)+\frac{4h^2}{R}+4\pi h\right]. \tag{4.3}$$

Assuming that the energy dissipated in the crushing process is equal to the potential energy of external forces:

$$E=P_m h \tag{4.4}$$

the expressions are derived for the mean crushing force P_m of the hat columns:

$$\frac{P_m}{M_0}=\frac{2\pi(a+b+4c)}{h}+\frac{4h}{R}+5\pi, \tag{4.5}$$

and of columns with square and rectangular cross sections:

$$\frac{P_m}{M_0}=\frac{2\pi(a+b)}{h}+\frac{4h}{R}+4\pi. \tag{4.6}$$

([1]) More details of calculations are given in Ref. [8].

Equations (4.5) and (4.6) can be minimized with respect to the parameter $h\left(\frac{d}{dh}(P_m(h))=0\right)$ which leads to the relation between geometrical parameters:

$$h^2=\frac{\pi}{2}R(a+b+4c), \tag{4.7}$$

$$h^2=\frac{\pi}{2}R(a+b) \tag{4.8}$$

for hat cross section columns and square and rectangular cross section columns, respectively. Substituing the relations (4.7) and (4.8) back into Eqs. (4.5) and (4.6), to eliminate the parameter R one gets simple expressions for the mean crushing force:

$$\frac{P_m}{M_0}=\frac{4\pi(a+b+4c)}{h}+5\pi \tag{4.9}$$

for hat cross section and

$$\frac{P_m}{M_0}=\frac{4\pi(a+b)}{h}+4\pi \tag{4.10}$$

for square and rectangular cross section columns.

The expressions (4.5)–(4.10) are obtained on the assumption that the shortening of the column δ is equal to h (wall thickness t equal to zero). In the real process the column shortening δ is smaller and equals

$$\delta=h-2t \tag{4.11}$$

(see Figs. 12 and 13).

Substituting this expression back into Eqs. (4.5)–(4.10), one gets the following expression:

$$P_m^*=\frac{P_m}{1-\frac{2t}{h}} \tag{4.12}$$

for all types of cross sections.

In view of the experimentally observed relation $h=b/4$ (see Ref. [1, 2, 3]), the following relations are obtained:

$$P_m^*=\frac{P_m}{1-\frac{2t}{h}}=16\pi\frac{\frac{a}{b}+4\frac{c}{b}+\frac{21}{16}}{1-8\frac{t}{b}}M_0, \tag{4.13}$$

for the hat cross section and

$$P_m^*=\frac{P_m}{1-\frac{2t}{h}}=16\pi\frac{\frac{a}{b}+\frac{20}{16}}{1-8\frac{t}{b}}M_0, \tag{4.14}$$

for the square and rectangular cross section; similar formulae can be derived for stresses:

$$\frac{\sigma_m^*}{\sigma_0}=\frac{2\pi\left(\frac{a}{q}+4\frac{c}{b}+\frac{21}{16}\right)}{\left(1-8\frac{t}{b}\right)\left(\frac{a}{t}+\frac{b}{t}+2\frac{c}{t}\right)}, \tag{4.15}$$

for the hat cross section and

$$\frac{\sigma_m^*}{\sigma_0}=\frac{2\pi\left(\frac{a}{b}+\frac{20}{16}\right)}{\left(1-8\frac{t}{b}\right)\left(\frac{a}{t}+\frac{b}{t}\right)}, \tag{4.16}$$

for the square and rectangular cross section, where σ_m^* denotes stresses resulting from the external force P_m^*:

$$\sigma_m^*=\begin{cases}\dfrac{P_m^*}{2(a+b+2c)t} & \text{for the hat cross section,}\\[2ex] \dfrac{P_m^*}{2(a+b)t} & \text{for the square rectangular cross section.}\end{cases} \tag{4.17}$$

It is interesting to compare the relative contribution of bending, rolling and corner type of deformation to the mean crushing force. In the case of the square cross section the contribution is respectively 44%, 44% and 12%.

5. Bending of closed section beams

The process of local buckling in thin-walled beams subjected to bending involves, as in the case of columns, the same three basic deformation mechanisms. The total increment of energy dE_c is thus equal to the sum of increments of energies due to bending, rolling and corner deformation

$$dE_c=dE_b+dE_r+dE_{cb}\,. \tag{5.1}$$

The energy E_c is computed by integrating Eq. (5.1) over the interval $[0, \Psi_e]$

$$E=\int_0^{\Psi_e} dE_c=\int_0^{\Psi_e} dE_b+\int_0^{\Psi_e} dE_r+\int_0^{\Psi_e} dE_{cb}\,, \tag{5.2}$$

where Ψ_e is the final rotation angle in a generalized plastic hinge. In the particular case of beams with a square cross section [2] the dE_c can be computed with the help of Eqs. (3.4) and (3.5), and Fig. 7.

$$dE_c(2\Psi)=M_0\,a\left\{(A-1)\left[6+\cos\alpha\left(\frac{2}{(2\lambda-\sin\alpha)\sqrt{\lambda^2-\lambda\sin\alpha}}+\right.\right.\right. \tag{5.3}$$

$$\left.\left.\left.+\frac{2\Phi}{\lambda}+\frac{2a}{\lambda^2 R}\right)\right]+A\left(2+\frac{2\sin\alpha}{\lambda}\right)+2\right\}d\Psi,$$

[2] Details of calculations are given in Ref. [9].

where

$$A=\frac{\lambda\cos\Psi}{\sqrt{\lambda\sin\Psi-\lambda^2\sin^2\Psi}},$$

$$\Phi=\arccos(1-2\lambda\sin\Psi),$$

$$\lambda=\frac{a}{b},$$

$\alpha=\Phi-\Psi$; a, b, Ψ are defined in Fig. 15.

Integrating Eq. (5.3) with respect to the angle Ψ_e, one gets

$$E_c(2\Psi_e)=M_0\left\{4a(2\Phi-\Psi)+2b\beta+2bD(b)+\frac{2b^2}{R}\sin\alpha\right\}, \tag{5.4}$$

where

$$D(b)=\int_0^{\Psi_e}\Phi\cos\alpha\,\alpha_{,\Psi}\,d\Psi+\int_0^{\Psi_e}\sin\alpha\,\Phi_{,\Psi}\,d\Psi,$$

$\Phi_{,\Psi}$, $\alpha_{,\Psi}$ denote derivatives with respect to the parameter Ψ.

The maximum angle through which the beam can be rotated forming a simple buckling wave is denoted by $2\Psi_e$. It is related to the geometrical parameters defined earlier by

$$\sin\Psi_e=\frac{b}{2a}=\frac{1}{2\lambda}, \tag{5.5}$$

see Ref. [9].

Defining the current and average bending moments respectively from the equality of internal and external increment of energies

$$\begin{aligned} dE_c&=M\,d(2\Psi),\\ E_c&=M_{av}\,2\Psi_e, \end{aligned} \tag{5.6}$$

the following formulae are obtained:

$$\frac{M(2\Psi)}{M_0\,a}=(A-1)\left[6+\cos\alpha\left(\frac{2}{(2\lambda-\sin\alpha)\sqrt{\lambda^2-\lambda\sin\alpha}}+\right.\right.$$
$$\left.\left.+\frac{2\Phi}{\lambda}+\frac{2a}{\lambda^2 R}\right)\right]+A\left(2+\frac{2\sin\alpha}{\lambda}\right)+2 \tag{5.7}$$

and

$$M_{av}(2\Psi_e)=\frac{M_0}{\Psi_e}\left\{4a(2\Phi-\Psi)+2b\beta+2bD(b)+\frac{2b^2}{R}\sin\alpha\right\}. \tag{5.8}$$

Equation (5.8) can be optimized with respect to the parameter b leading to the relation between the geometrical parameters

$$\frac{a}{R}=\frac{\pi+\beta\sin\Psi-(\beta_{,\Psi}\sin\Psi-\beta\cos\Psi)\Psi}{2[2(\sin\Psi\cos^2\Psi-\sin^3\Psi)\Psi-\sin^2\Psi\cos\Psi]}. \tag{5.9}$$

Substituting this relation back into Eq. (5.7) to eliminate parameter R and setting the experimentally observed value $\lambda=1$ (see also Ref. [5]), one gets the following expression:

$$\frac{M(2\Psi)}{M_0 a}=(A-1)\left[6+\cos\alpha\left(\frac{2}{(2-\sin\alpha)\sqrt{1-\sin\alpha}}+2\Phi+26.2\right)\right]+ \tag{5.10}$$

$$+2A(1+\sin\alpha)+2,$$

where, according to Eq. (5.3), all parameters are expressed in terms of the angle Ψ.

Equation (5.10) provides a relatively simple closed form solution for the bending resistance of box section beams. A typical plot of the function $M(2\Psi)$ is shown in Fig. 24. It should be mentioned that a similar solution was obtained by TIDBURY and KECMAN [5, 15] on the basis of a different collapse mechanism which does not involve the corner deformation. However, in the present paper the rolling radius has been eliminated by means of the minimization procedure. The formulae described in Refs. [5] and [15] involved the rolling radius whose value had to be taken from experimental observations.

6. BENDING OF THE U-SECTION BEAMS

Similar considerations, as those presented in Sects. 4 and 5, lead to the formulae describing the bending resistance in the case of "outward" and "inward" bending of U-section beams. Thus we obtain [3]

$$\frac{M(2\Psi)}{M_0 c}=\frac{\cos\alpha\,\alpha_{,\Psi}\,\mu}{\lambda}\left(4\frac{b}{R}+2\Phi\right)+\Phi_{,\Psi}\left(\frac{2\mu\sin\alpha}{\lambda}+4\mu+4\right)-4\mu-1, \tag{6.1}$$

$$\mu=\frac{a}{c},\qquad \lambda=\frac{a}{b},$$

(see Fig. 15) for "outward bending" and

$$\frac{M(\varphi)}{M_0 c}=\frac{4\mu}{\cos\alpha}\beta_{,\varphi}+2\mu\Phi_{,\varphi}+1, \tag{6.2}$$

$$\mu=\frac{a}{c}$$

(see Fig. 16) for "inward bending". The extremum condition yields the following relation for the "outward bending":

$$\frac{a}{R}=\left(1+\frac{1}{\mu}\right)3.49, \tag{6.3}$$

---

[3] More details are given in Ref. [9].

in which the approximate relation $\lambda=1$ was used. In the case of the "inward bending" optimization of Eq. (6.2) with respect to the parameter α yields

$$\cos^2\alpha-\alpha\sin\alpha+\cos\alpha=0, \tag{6.4}$$

whose solution is $\alpha\approx 57°$.

Here the collapse mechanism is determined to within a single parameter α which is uniquely found from Eq. (6.4) Substituting the relations (6.3) and $\alpha=57°$, respectively to the formulae (6.1) and (6.2) one gets the final relations for the strength of the *U*-section beams in bending:

$$\frac{M(2\Psi)}{M_0 c}=0.94\mu\cos\alpha_{,\Psi}\left[13.6\left(1+\frac{1}{\mu}\right)+2\Phi\right]+ \tag{6.5}$$

$$+\Phi_{,\Psi}(1.87\mu\sin\alpha+4\mu+4)-4\mu-2$$

for "outward bending" and

$$\frac{M(\varphi)}{M_0 c}=\frac{\mu}{\cos^2\left(57°-\frac{\varphi}{2}\right)}\left(\frac{2.380}{\sqrt{1-0.420\,\mathrm{tg}^2\left(57°-\frac{\varphi}{2}\right)}}+\right. \tag{6.6}$$

$$\left.+\frac{1.300}{\sqrt{1-0.106\,\mathrm{tg}^2\left(57°-\frac{\varphi}{2}\right)}}\right)+1$$

for "inward bending" of the *U*-section beams.

7. Comparison with experimental data

7.1. Crushing of columns

In order to validate the present theory, results of experiments reported in Refs. [1, 2, 3, 12, 13] will be used. In particular, comparison will be made with the experimental data obtained by Ohokubo *et al.* [1] and Aya *et al.* [2]. Ohokubo has performed a series of tests on mild steel columns ($\sigma_0=0.25$ GPa) with hat cross sections and gauge thickness ranging from 1.2 to 2.0 mm (Fig. 20). Mild steel hat columns with equal lengths of both sides ($a=b$) and variable thickness 1–3.5 mm were tested by Aya et al. (Fig. 21). The measured yield stress was $\sigma_0=$ $=0.22$ GPa. The present theoretical solutions (formulae (4.13)) are shown in Figs. 20 and 21 in solid lines.

Using the dimensionless variables defined by Eq. (4.17), it is possible to compare the results of all the above mentioned experimental data with the prediction of the formulae (4.15) and (4.16) (Fig. 22). It is seen that the difference between experiments and theory never exceeds 20%. The obtained agreement should be regarded as good considering the fact that scatter of experimental data is of the order 10% and the yield stress of the material is determined to within 10–15%.

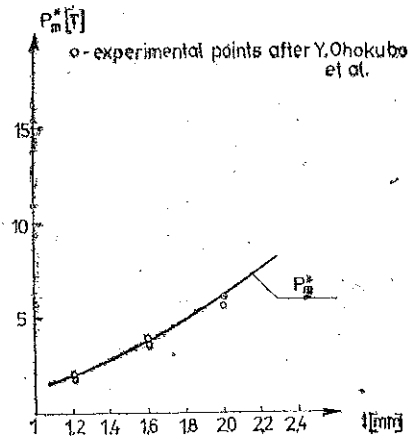

FIG. 20. Plot of the mean crushing force (Eq. (4.13)) versus gauge thickness.

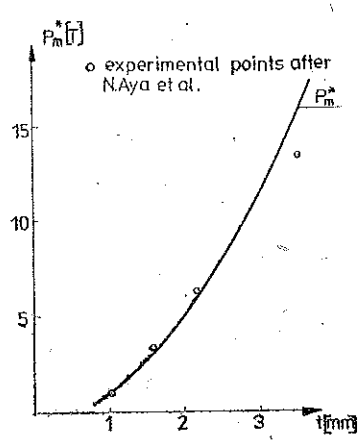

Fig. 21. Plot of the mean crushing force (Eq. (4.13)) versus gauge thickness.

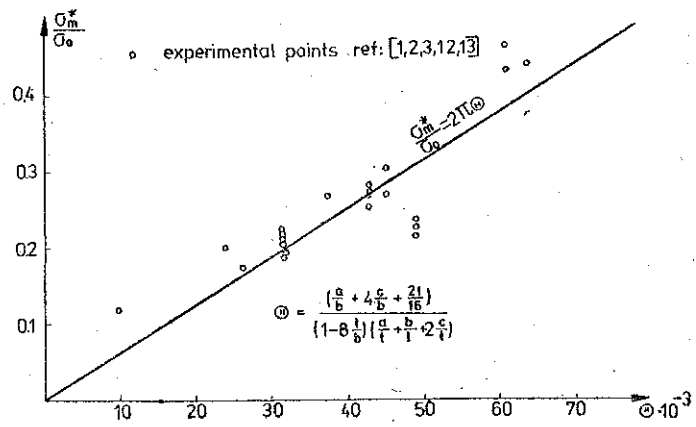

FIG. 22. Plot of the ratio σ_m/σ_0 in the present theoretical solution (Eq.(4.15)) versus dimensionless parameter Θ.

There are other methods of evaluating experimentally the mean crushing strength and energy absorption of thin-walled columns and a critical review of these methods was recently presented by Thornton [13].

In order to compare energy absorption capability of various structures, Magee and Thornton ([16]) introduced two new functions: the structural effectiveness η and relative density (solidity ratio) Φ. The structural effectiveness is defined by

$$E_s^c=\eta\sigma_u^s, \tag{7.1}$$

where $E_s^c=E_c/V\rho$ is the specific energy, i.e. energy divided by the weight of the structure, $\sigma_u^s=\sigma_0/\rho$ is the specific tensile strength, V denotes the volume of the structure and ρ is the mass density of the material. The relative density Φ is a ratio of the cross section area of the tube to the cross section area of the solid of the same outer dimensions.

Magee and Thornton in a series of recent papers [17, 16, 18] found empirical relations between η and Φ for a variety of tube cross sections by fitting a large number of experimental points.

It appears that the formula (4.9) for the mean crushing strength of columns with hat cross sections can be related to η and Φ if some approximations are introduced. One can show that a lower bound for η obtained from Eq. (4.9) is

$$\eta=\frac{\pi}{2\left(1+\frac{c}{a}\right)}\Phi, \tag{7.2}$$

which, depending on the magnitude of the ratio t/a, underestimates the exact solution by some 10%.

In the case of columns with a square cross section $a=b$, the formula (4.3) can be expressed in terms of η and Φ without any simplifying assumptions:

$$\eta=\frac{9\pi}{16}\Phi, \tag{7.3}$$

The above expression is also a valid approximation for rectangular columns with the ratio $a/b=1\div 2$. A solid line in Fig. 23 corresponds to the theoretical solutions (7.2) and (7.3). The experimental points have been collected in Ref. [13]. As before, the correlation between theory and experiments should be considered as good.

7.2. Bending of beams

The experimental results with which the present theoretical solution is compared are due to Kecman [15] and Titbury and Kecman [5]. The dimensions of the tested mild steel beams were $a\times b\times t=100\times 100\times 0.914$ mm and the yield stress was equal to $\sigma_0=0.22$ GPa. The angle 2Ψ ranged from 0° to 10°. Figure 24 shows a comparison of the measured bending moment-angle rotation relationship with the prediction of the present solution [formula (5.10)]. The agreement is generally

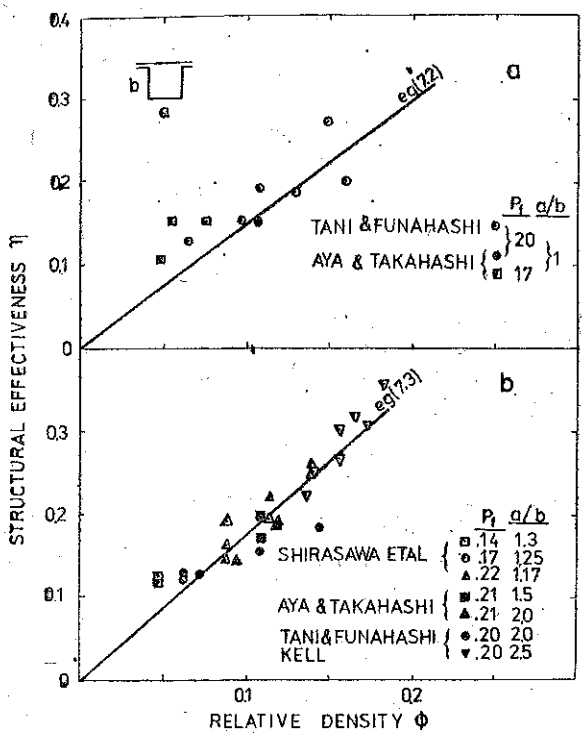

FIG. 23. Comparison of the present theoretical solution (Eqs. (7.2) and (7.3)) with experimental data.

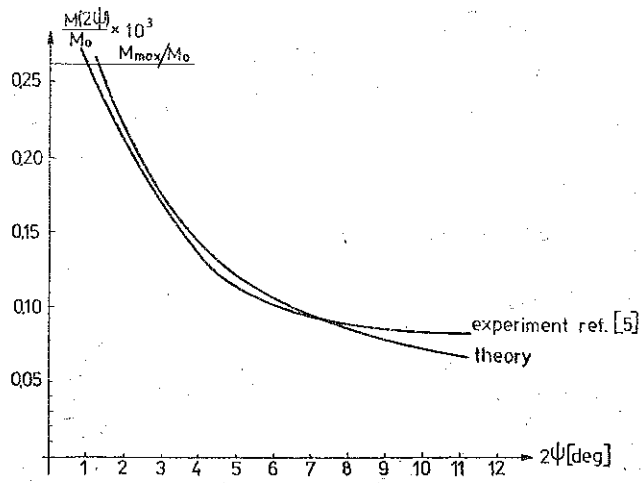

FIG 24 Comparison of the present theoretical solution (Eq. (5.10)) with experimental data.

good except for very small angles. The present simplified analysis which disregards the bending moments-membrane forces interactions gives an infinite value of the bending moment with 2Ψ approaching zero. Therefore the $M(2\Psi)$ diagram has been truncated by the horizontal line representing the so-called fully plastic bending moment of the cross section.

It can be concluded that the presented theoretical method leads to results which are simple and sufficiently accurate for practical applications.

REFERENCES

1. Y. OHOKUBO, T. AKAMATSU and K. SHIRASAWA, *Mean crushing strength of closed-hat section, members*, SAE paper, 740040.
2. N. AYA and K. TAKAHASHI, *Energy-absorbing characteristics of vehicle body structure*, Part I, Trans. of the Society of Automotive Engineers of Japan, **7**, 1974.
3. T. AKERSTRÖM and T. WIERZBICKI, *Dynamic crushing of strain rate sensitive box columns*, Proc. 2-nd International Conference of Vehicle Structural Mechanics, Michigan 1977.
4. M. YAMAYA and M. TANI, *Energy absorption by the plastic deformation of sheet metal column with box-shaped cross section*, Mits. Techn. Rev., **8**, 1, 1971.
5. G. H. TIDBURY and D. KECMAN, *Investigation into behaviour of hinges produced by bending collapse of vehicle structural components*, Proc. XVIII Congress International FISITA, II, Budapest 4–10 June 1978.
6. N. SEKI and Y. SUNAMI, *Energy absorption of thin-walled box subjected to combination of bending with axial compression*, Proc. XVIII Congress International FISITA, II, Budapest 4–10 June 1978.
7. J. K. MC IVOR, W. J. ANDERSON and M. BIJAK-ZOCHOWSKI, *An experimental study of the large deformation of plastic hinges*, The University of Michigan Rep. 48109.
8. W. ABRAMOWICZ, *Energy absorption of thin-walled metal columns* (in Polish), Institute of Fundamental Technological Research, Technical Report, 19, 1979.
9. W. ABRAMOWICZ, *Simplified analysis of thin-walled beams with closed and open cross-sections*, (in Polish) Institute of Fundamental Technological Research, Technical Report, **56**, 1979.
10. A.V. POGORIELOV, *Bending of convex surfaces*, (in Russian), Moscow 1951.
11. A.V. POGORIELOV, *Geometrical methods in nonlinear theory of elastic shells*, (in Russian), Izd. Nauka, Moscow 1967.
12. W. ABRAMOWICZ and A. ŻUKOWSKI, *Energy absorption of thin-walled metal columns — comparison with experimental data*, Technika Motoryzacyjna, 1980 (to appear).
13. P. H. THORTON, *Energy absorption by the structural collapse of spot-welded sheet metal sections*, Ford Research Technical Report, SR 79–52.
14. P. H. THORTON, *The collapse of square section tubes in bending*, Ford Research Technical Report, SR 79–06.
15. D. KECMAN, *Bending collapse of rectangular section tubes in relation to the bus roll-over problem*, Cranfield Institute of Technology Ph.D. Thesis, 1979.
16. P. H. THORTON, *Energy absorption by foam-filled structures*, Ford Research Technical Report, SR 79–82.
17. P. H. THORTON, *Energy absorption by structural collapse*, Ford Research Technical Report, SR 79–83.
18. P. H. THORTON and C. L. MAGEE, *The interplay of geometric and materials variables in energy absorption*, Trans. ASME, pp. 114–120, April 1977.

STRESZCZENIE

KINEMATYCZNA ANALIZA ZGNIATANIA CIENKOŚCIENNYCH KOLUMN METALOWYCH

Podano przybliżoną analizę wyznaczania energochłonności cienkościennych belek i kolumn metalowych o przekrojach kwadratowym, prostokątnym, kapeluszowym i ceowym poddanych quasi-statycznemu zgniataniu i zginaniu. Opisano trzy podstawowe mechanizmy deformacji i obliczono odpowiadające im przyrosty rozpraszanej energii i wyznaczono średnią siłę ścinającą dla wszystkich typów konstrukcji. Otrzymano dobrą zgodność wyników doświadczalnych i obliczeniowych.

Резюме

КИНЕМАТИЧЕСКИЙ АНАЛИЗ СДАВЛИВАНИЯ ТОНКОСТЕННЫХ МЕТАЛЛИЧЕСКИХ КОЛОНН

Приведен приближенный анализ определения энергоемкости тонкостенных балок и металлических колонн, с квадратным, прямоугольным, шляпообразным и швеллерным сечениями, подвергнутых квазистатическому сдавливанию и изгибу. Описаны три основных механизма деформации и вычислены отвечающие им приросты рассеиваемой энергии, а также определена средняя сила сдвига для всех типов конструкций. Получено хорошее совпадение экспериментальных и расчетных результатов.

POLISH ACADEMY OF SCIENCES
INSTITUTE OF FUNDAMENTAL TECHNOLOGICAL RESEARCH

Received February 15, 1980.